Spline-based Trajectory Planning Techniques for Benthic AUV Operations

Kiran Murthy* and Stephen Rock*†
kmurthy@stanford.edu, rock@stanford.edu

*Dept. of Aeronautics and Astronautics
Stanford University
496 Lomita Mall
Stanford, CA 94305

†Monterey Bay Aquarium Research Institute
7700 Sandholdt Road
Moss Landing, CA 95039

***Abstract*—AUVs increasingly are being used to collect data in the benthic environment. Many of these data collection tasks require that the AUV is able to follow the terrain at standoff distances on the order of meters (e.g. benthic imaging). However, terrain following with an AUV is a challenging problem when the terrain is rough, and the task becomes even more difficult when using motion-constrained vehicles such as torpedo-style AUVs. One option to improve the terrain-following capability of these vehicles is to incorporate a trajectory following control law. This requires, however, the generation of a trajectory. This paper presents a spline-based trajectory planning technique that exploits prior knowledge of terrain shape and explicitly takes motion constraints into consideration.**

Details of a the trajectory planning method are provided. The method forms terrain following trajectories by using a spline-based representation of the underlying terrain. A vehicle turning radius constraint along the trajectory is mapped to spline surface curvature constraints by leveraging the continuous nature of the spline-based terrain representation. A curvature-constrained spline surface is then fit to bathymetry by solving an optimization problem. If a feasible solution does not exist, the AUV is not able to survey the site under the specified turning radius constraint. Consequently, this method can also be used as a design tool to determine an AUV's actuation requirements to survey a given terrain.

Examples of planned trajectories for an MBARI *Dorado* AUV over Monterey Bay bathymetry are provided.

I. Introduction

AUVs play an important role in obtaining many different types of data on the ocean floor. Examples include benthic imagery and sonar data [1], [2]. These data sets are obtained by having the AUV follow the terrain's shape while pointing the instrument (camera or sonar sensor) toward the terrain. Although this operation has been performed by maneuverable AUVs [2], the task becomes much more challenging when using a motion-constrained AUV to survey rough terrain.

One of the challenges of collecting images or sonar data over rough terrain stems from a desire for instrument-terrain perpendicularity. The perpendicularity is desired because the collected data is of higher quality when the instrument is pointed perpendicular to the terrain. During image collection, camera-terrain perpendicularity minimizes the perspective distortion seen in the images, reducing the need to remove this distortion in post-processing [3]. When collecting sonar data, the highest-accuracy data is collected when the sonar beam is perpendicular to the terrain [4].

Although highly maneuverable AUVs can achieve perpendicularity by sensing and reacting to terrain orientation changes (such as [5], [2]), motion-constrained AUVs (i.e. torpedo-style AUVs) may have difficulty maintaining perpendicularity over rough terrain. In particular, torpedo-style AUVs typically have an actuation scheme that results in a minimum turning radius constraint. Since this motion constraint limits the speed at which the AUV can react to terrain changes, it is desirable to have feed forward information on the upcoming terrain's shape (see Figure 1).

This feed forward capability can be provided by planning a desired AUV trajectory over the survey area, then having the AUV's control system follow the desired trajectory. This paper proposes a method that plans AUV survey trajectories while accounting for AUV motion constraints. The trajectory planning tool uses terrain data to plan smooth survey trajectories for turning radius-constrained vehicles that maintain instrument-terrain perpendicularity. The trajectories are planned by computing a spline surface-based representation of the terrain over which trajectory curves are generated (see Figure 2). Turning radius constraints are explicitly dealt with by way of curvature constraints on the spline-based terrain representation.

Results are presented that show survey trajectories in Monterey Bay that adhere to the MBARI *Dorado* vehicle's turning radius constraint.

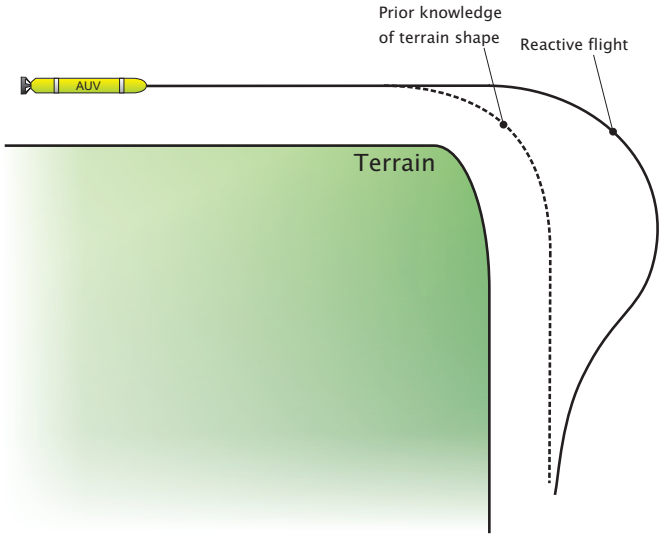

Fig. 1. An AUV with prior knowledge of terrain shape can react to terrain changes before sensing the change. This mechanism allows a turning radius constrained AUV to maintain better instrument-terrain perpendicularity over rough terrain.

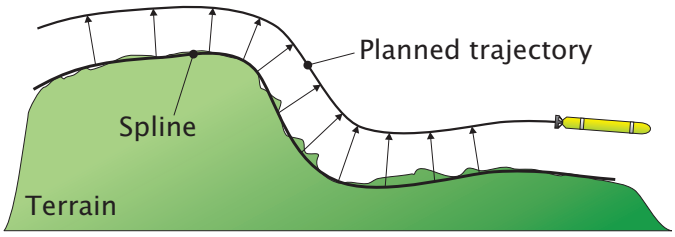

Fig. 2. The vehicle's trajectory is planned by using a spline-based representation of the terrain. The planned trajectory must adhere to the vehicle turning radius constraint, which limits the maximum curvature of the spline.

II. Background

A. AUV-Based Benthic Surveys

Instrument terrain perpendicularity can be achieved in different ways depending on the maneuverability of the AUV. Highly maneuverable AUVs can survey terrain by reacting to terrain changes, and their primary hurdle to achieving perpendicularity is determining the terrain's orientation. Examples of such AUVs are DEPTHX [6] and the Bluefin HAUV-1B [7]. These AUVs achieve instrument perpendicularity by closing a control loop to point the instrument normal to the sensed terrain orientation. Acoustic sensors are used to determine the orientation of the surface being surveyed. When operating close to the terrain, high spatial frequencies in the terrain (e.g. rocky outcroppings) detected by the sensors are smoothed using various methods of spatial filtering. DEPTHX performs spatial filtering by fitting a plane to the n most recent range measurements instead of only the requisite three measurements. An alternative spatial filtering technique that can leverage prior knowledge of terrain shape is a spline-based spatial filter [8].

Due to their turning radius constraint, torpedo-style AUVs are limited in their ability to react to terrain changes. Consequently, these AUVs have typically been used to perform visual surveys over smooth terrain and sonar surveys [1] at a high altitude.

Incorporating a pre-planned trajectory can improve performance over rough terrain. In particular, when operating within visual range of rough terrain, prior knowledge of terrain shape is important in maintaining perpendicularity, and this prior knowledge can be captured by a pre-planned trajectory. Planning a trajectory can also help produce higher-quality sonar surveys by allowing the AUVs to fly a constant altitude over the terrain. These constant altitude trajectories lead to a sonar data set with uniform accuracy.

The work proposed in this paper addresses how to leverage prior knowledge of terrain shape to plan trajectories for motion-constrained AUVs that maintain instrument-terrain perpendicularity. The trajectories can then be driven by the AUV using a number of different trajectory following control systems [9], [10].

B. Related AUV Trajectory Planning Techniques

There is an abundance of work in AUV trajectory planning, but none of the methods extend to flying torpedo-style AUVs while maintaining instrument-terrain perpendicularity. AUV trajectory planning can occur online in response to sensor data or offline before the AUV mission. An example of online trajectory planning is the method used by the hover-capable SeaBED-class AUV, which has performed visual surveys in many different locations [11], [12], [13]. This AUV achieves perpendicularity by using a terrain following algorithm that attempts to maintain a constant altitude above the terrain. The algorithm uses sensor data and a simple dynamic model of the AUV to generate a feasible reference trajectory, which is then fed to the control system. The use of the dynamic model accounts for the vehicle's actuation constraints. However, SeaBED's trajectory generation algorithm may not translate well to torpedo-style AUVs since it does not use *a priori* terrain shape information when computing the reference trajectory. To maximize perpendicularity, the trajectories planned for turning radius constrained AUVs must begin reacting to a terrain change before the altimeter senses the change.

Offline trajectory planning for underactuated AUVs is a well-studied field. The objectives of previous offline trajectory planners include obstacle/terrain avoidance [14], satisfying vehicle motion constraints [9], navigating a series of 2-D waypoints [15], and attaining maximum coverage over a site [14], [16]. However, the previous work does not explicitly account for perpendicularity during the trajectory planning process. The work in this paper addresses instrument-terrain perpendicularity as the primary objective of the planned trajectory.

C. Related Work in Other Fields

The problem of flying trajectories that maintain perpendicularity draws parallels to work in other fields. There is a large body of work in the computer graphics community

regarding navigation in virtual environments. Part of this work is focused on pointing the camera toward a surface while moving through the virtual environment [17], [18], [19], [20]. An algorithm by Autodesk Research called HoverCam [19] achieves camera perpendicularity by pointing the camera at the closest point on the surface at all times. The spline-based terrain representation presented in this paper is a compatible approach. The compatibility exists since the closest point on the spline-based terrain representation to the vehicle position is easy to find via the spline point projection algorithm.

A large body of work in offline trajectory planning also exists in other fields. Specifically, the study of nap-of-the-earth flight has produced many different terrain following trajectory planning techniques for aircraft and rotocraft [21], [22], [23]. Though much of this work accounts for vehicle actuation constraints while following the shape of the terrain, the trajectory planners optimize for maximum speed instead of terrain perpendicularity [23].

III. Trajectory Planning Method

The trajectory planning method produces a desired AUV trajectory that achieves instrument-terrain perpendicularity. The method uses terrain shape information and accounts for a vehicle turning radius constraint in order to produce the trajectory.

The trajectory planning method produces a 3-D curve that defines a survey trajectory between a start and end location over the terrain. The algorithm produces the curve by using a spline-based terrain representation that is computed by solving the optimization problem defined in Figure 3.

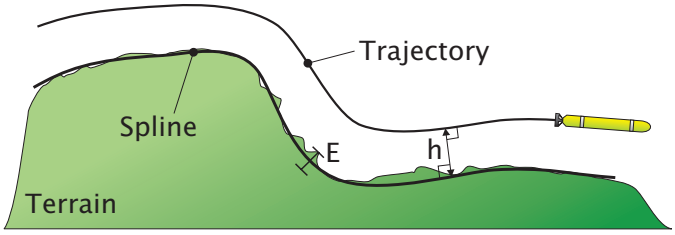

Fig. 3. The trajectory planning problem.

That is, given the terrain data in the form of a Digital Elevation Model (DEM), survey altitude h, and the vehicle's minimum turning radius R_{min}, the optimization problem finds a spline surface that best fits the terrain within a maximum error E. This maximum error is chosen such that the altitude of the trajectory remains within desired bounds around the nominal survey altitude h. In addition, curvature constraints are imposed upon the spline surface. Since the trajectory and spline are mutually perpendicular at a distance h and the maximum curvature of the trajectory must be $\frac{1}{R_{min}}$, the spline's curvature must also be constrained.

$$\text{Given:} \begin{cases} \text{Terrain data (DEM)} \\ h \text{ (survey altitude)} \\ E \text{ (max fitting error)} \\ R_{min} \text{ (vehicle minimum turning radius)} \end{cases}$$

$$\underset{\text{Spline}}{\text{minimize}} \quad [\text{Fitting error (error between spline and terrain data)}]$$

$$\text{subject to} \quad \text{Fitting error} \leq E$$

$$\begin{cases} \text{Trajectory and spline are mutually perpendicular} \\ \text{Trajectory radius of curvature} \geq R_{min} \end{cases}$$

or equivalently

$$\begin{cases} \text{Spline curvature} \leq \kappa_{max} = f(h, R_{min}) \end{cases}$$

The constrained spline surface is fit to terrain data by solving a nonlinear optimization problem. The problem is posed such that it can quickly be solved using a Sequential Quadratic Programming (SQP) solver.

A. Constraints on Spline-based Terrain Representation

Since the planned trajectory is derived from the shape of the spline-based terrain representation, vehicle motion constraints can be mapped to constraints on the spline surface. In particular, the vehicle turning radius constraint is mapped to a constraint on the spline surface's curvature.

Consider a vehicle flying over a circular section of spline with radius R_s at a given altitude h. The relationship between R_s and the turning radius of the vehicle trajectory R_t is different depending on whether the spline section is convex or concave with respect to the vehicle (see Figures 4 and 5).

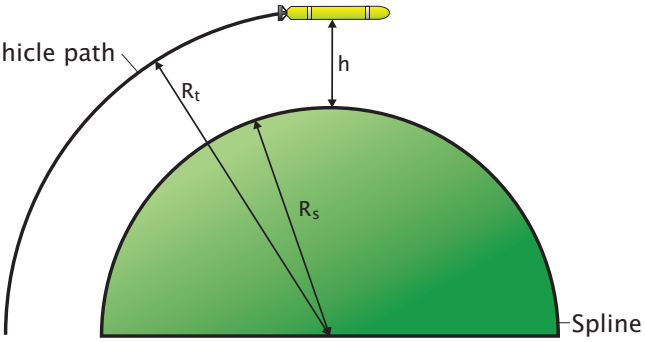

Fig. 4. Vehicle trajectory over convex circular spline. The vehicle's turning radius is greater than the radius of the spline.

If the section of spline is convex:

$$R_t = R_s + h \tag{1}$$

If the section of spline is concave:

$$R_t = R_s - h \tag{2}$$

Defining the vehicle's minimum turning radius as R_{min}, the vehicle's turning radius constraint can be expressed as $R_t \geq$

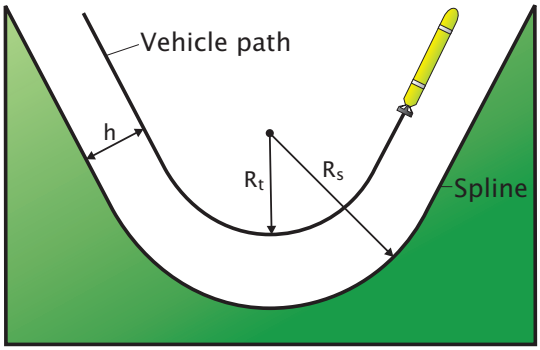

Fig. 5. Vehicle trajectory over concave circular spline. The vehicle's turning radius is less than the radius of the spline.

R_{min}. Applying this relation yields two inequalities that relate R_{min} to R_s:

$$R_s \geq R_{min} - h \tag{3}$$

$$R_s \geq R_{min} + h \tag{4}$$

If the spline's radius of curvature R_s satisfies Equation 4, then Equation 3 is automatically satisfied. Thus, only one constraint on the spline's curvature $\kappa_s = \frac{1}{R_s}$ is needed and can be derived from Equation 4:

$$\kappa_s \leq \frac{1}{R_{min} + h} = \kappa_{max} \tag{5}$$

By choosing to constrain the spline's curvature based only on the concave constraint, the final trajectory's shape is restricted to a "worst case" scenario where the terrain is concave everywhere. Different curvature constraints could be applied to different regions of the spline based on the spline's convexity, allowing the resulting trajectories to follow convex regions of the terrain more closely. However, adding the additional conditional constraints would significantly complicate the problem.

A maximum fitting error constraint E is also imposed upon the spline, which restricts the maximum distance between the spline surface and the terrain data to be below E. In this manner, if an AUV flies a trajectory h meters above the spline, the actual vehicle altitude will be bounded between $[h - E, h + E]$.

B. Nonlinear Optimization Problem

The goal of the nonlinear optimization problem is to find a set of spline control points $\mathbf{P}$ that control the shape of the spline surface. The control points $\mathbf{P}$ are computed in order to minimize the fitting error between the spline and terrain data. In addition, the optimization takes into account the aforementioned curvature constraints and the maximum fitting error constraint.

The nonlinear optimization problem is set up by starting with the unconstrained spline fitting optimization problem, then adding the curvature constraints. The tensor product B-spline surface maps a parameter domain (u, v) to 3-D points $\mathbf{S}$. The spline surface equation is:

$$\mathbf{S}(u,v) = \sum_{j=0}^{n} \sum_{k=0}^{m} N_{j,p}(u) N_{k,p}(v) \mathbf{P}_{j,k} \tag{6}$$

The mapping between (u, v) and $\mathbf{S}$ is performed by taking linear combinations of control points $\mathbf{P}_{j,k}$. The coefficients for the linear combination derived by evaluating p-th degree piecewise polynomial basis functions $N_{j,p}$ and $N_{k,p}$ at specific (u, v) pairs. The work in this paper uses third degree (cubic) spline surfaces.

Given a (u, v) pair, the relation between the associated point on the surface $\mathbf{S}(u, v)$ and the control points $\mathbf{P}_{j,k}$ and is linear. This linear relationship can be written in matrix-vector form:

$$\mathbf{S}(u,v) = N(u,v)P \tag{7}$$

where $N(u, v)$ is a matrix of products of spline basis function evaluations at (u, v) and P is a vector formed from the control point locations.

The unconstrained spline fitting optimization problem makes use of this linear map between control points and points on the spline surface. Each data point $\mathbf{D}_l$ is given an associated (u_l, v_l) parameter pair on the spline surface using one of many well known methods [24]. The goal of spline fitting is to find the control points that minimize the distance between the data points and the associated (u, v) point on the spline surface. The spline fitting problem can be expressed as the following optimization problem:

$$\underset{P}{\text{minimize}} \quad ||NP - D|| \tag{8}$$

where D is a vector of concatenated data points and N is a matrix given by the following relation:

$$N = \begin{bmatrix} N(u_1, v_1) \\ N(u_2, v_2) \\ \vdots \\ N(u_n, v_m) \end{bmatrix}$$

Various curvature metrics can be used to add curvature constraints to this optimization problem. For simplicity, the curvature along isoparametric curves on the spline surface is constrained. This constraint is an approximation that will limit the spline surface's curvature along the two parametric directions of the surface. However, the curvature in non-parametric directions is not constrained, and trajectories traveling in non-parametric directions may not adhere to the vehicle's turning radius constraint.

The curvature of an isoparametric curve in parameter direction u at a parameter pair (u, v) is given by:

$$\kappa_u(u,v) = \frac{||\mathbf{S}_u \times \mathbf{S}_{uu}||}{||\mathbf{S}_u||^3}, \quad \mathbf{S}_u = \frac{\partial \mathbf{S}(u,v)}{\partial u} \tag{9}$$

$$\mathbf{S}_{uu} = \frac{\partial^2 \mathbf{S}(u,v)}{\partial u^2}$$

Instead of enforcing this constraint at many (u, v) locations, a property of cubic B-spline surfaces allows the number of constraints to be reduced. The second derivative $\mathbf{S}_{uu}$ of a cubic spline surface's isoparametric curve is piecewise linear with maxima at known parameter locations (u_i, v_i). As a result, the isoparametric curvature κ_u is nearly piecewise linear with maxima near the second derivative maxima. Thus, constraining curvature at the known second derivative maxima will constrain isoparametric curvature for nearly the entire spline surface.

The following curvature constraints are desired at the second derivative maxima (u_i, v_i):

$$\kappa_u(u_i, v_i) \leq \kappa_{max}, \ \forall(u_i, v_i)$$
$$\kappa_v(u_i, v_i) \leq \kappa_{max}, \ \forall(u_i, v_i)$$

The curvature expression in Equation 9 involves a nonlinear cross product operator. The expression can be simplified as follows:

$$\begin{aligned}\kappa_u &= \frac{||\mathbf{S}_u \times \mathbf{S}_{uu}||}{||\mathbf{S}_u||^3} \\ &= \frac{||\mathbf{S}_u|| \cdot ||\mathbf{S}_{uu}|| \cdot |\sin\theta|}{||\mathbf{S}_u||^3} = \frac{||\mathbf{S}_{uu}|| \cdot |\sin\theta|}{||\mathbf{S}_u||^2} \\ &\leq \frac{||\mathbf{S}_{uu}||}{||\mathbf{S}_u||^2} \leq \kappa_{max}\end{aligned} \tag{10}$$

Similar to Equation 7, there exists a linear relationship between the spline control points and derivatives of the spline:

$$\mathbf{S}_u(u, v) = A_u(u, v)P$$
$$\mathbf{S}_{uu}(u, v) = B_u(u, v)P$$

By substituting this linear relationship into Equation 10 and including the maximum fitting error constraint $||NP - D|| \leq E$, the constrained spline fitting problem can be expressed as:

$$\begin{aligned}\underset{P}{\text{minimize}} \quad & ||NP - D|| \\ \text{subject to} \quad & \frac{||B_u^{(i)}P||}{||A_u^{(i)}P||^2} \leq \kappa_{max} \ \forall(u_i, v_i) \\ & \frac{||B_v^{(i)}P||}{||A_v^{(i)}P||^2} \leq \kappa_{max} \ \forall(u_i, v_i) \\ & ||NP - D|| \leq E\end{aligned} \tag{11}$$

The SQP method provides an efficient way to solve this optimization problem. During each optimization iteration, the SQP method makes use of the Hessian of the optimization problem's Lagrangian to compute a step to take [25]. Squaring all of the individual expressions in Equation 11 yields an equivalent optimization problem containing quadratic expressions. These quadratic expressions allow the Hessian of the Lagrangian to be computed in closed form, enabling the SQP method to compute steps during optimization iterations quickly.

If the SQP optimization solver cannot find a feasible solution, the terrain contains too much variation to be surveyed by the turning radius constrained vehicle within the specified altitude bounds.

C. Final Trajectory Generation

After a curvature-constrained spline surface is fit to terrain data, 3-D trajectory curves that adhere to the turning radius constraint and altitude bounds can be derived from the spline. Though there are many ways to draw the actual trajectory, a straightforward method is to compute a set of points on the spline, then move the points along the spline surface normal at each point. The resulting points can then be interpolated using a cubic spline, yielding a continuous trajectory curve.

The trajectory's start and end locations are specified by two (u, v) parameters on the spline-based terrain representation. Linearly interpolating between the start and end parameters yields a series of parameter pairs (u_t, v_t). Each of these parameter pairs is associated with a point on the spline (see Figure 6).

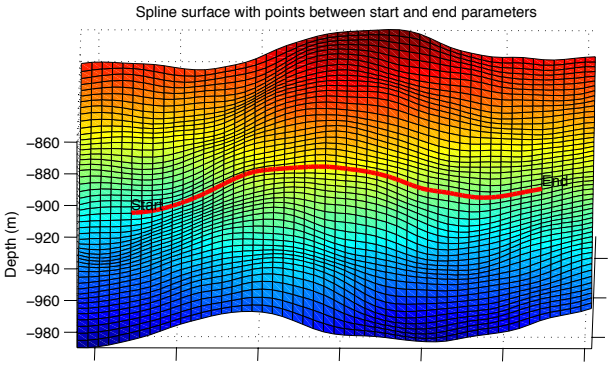

Fig. 6. Points on a spline surface lying at parameter values linearly interpolated between the start and end (u, v) parameter pairs.

To compute points on the trajectory, the points on the spline at the (u_t, v_t) parameters are moved by the survey altitude in the direction of the spline surface normal at each (u_t, v_t) projected into the plane of the trajectory (see Figure 7). The points on the trajectory are then interpolated using a B-spline curve, resulting in a continuous function that represents the desired vehicle trajectory. The continuous nature of the trajectory is advantageous when an AUV is attempting to follow the trajectory with a control system. The advantage stems from the ability to compute the curvature of the trajectory close to the AUV's current location quickly, allowing the AUV to have feed-forward information about how fast the vehicle should be turning.

IV. Results

The presented trajectory planning method was executed over two Monterey Bay bathymetry data sets. The data sets are

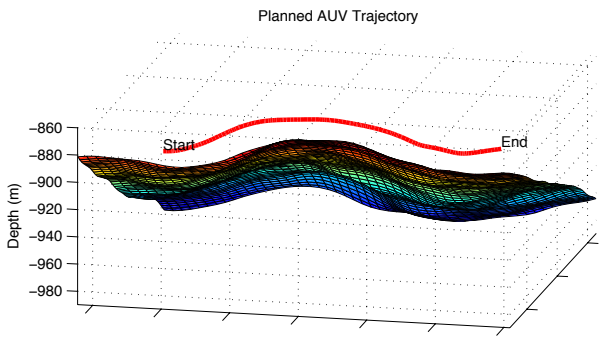

Fig. 7. Points on spline have been moved by survey altitude along spline surface normals, yielding points on the desired AUV survey trajectory.

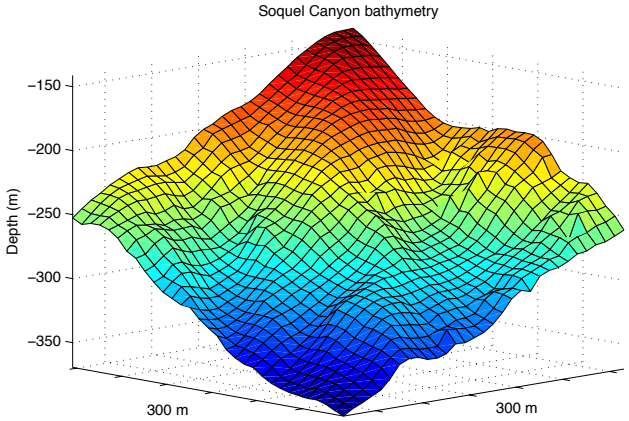

Fig. 9. Bathymetry around Soquel Canyon waypoint. The data is spaced on a 10 m grid.

centered on two waypoints in Monterey Bay named "Clam Field South" and "Soquel Canyon #4" (see Figures 8 and 9) The Soquel Canyon site contains rougher terrain with higher curvature than Clam Field South.

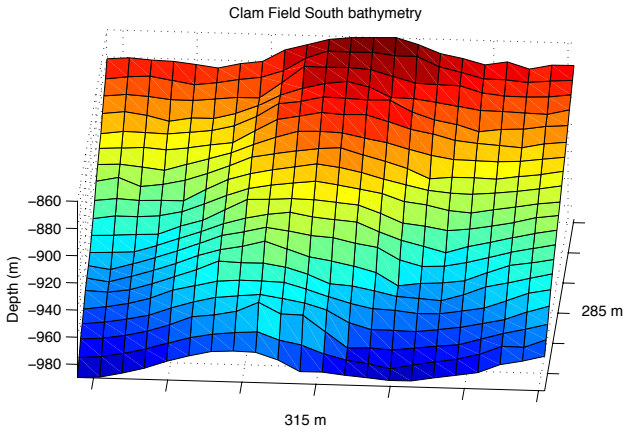

Fig. 8. Bathymetry around Clam Field South waypoint. The data is spaced on a 15 m grid.

The trajectories were planned for an MBARI *Dorado* class AUV (see Figure 10) surveying the terrain at two different altitudes. The *Dorado* is a torpedo-style AUV that has has a minimum turning radius of 10 m (typical). Trajectories were planned for two different characteristic surveys. A visual survey requires the vehicle to be within visual range of the terrain, so the nominal survey altitude was set at 5 m with altitude bounds set at +/- 2 m. In a large-area sonar based data collection survey, the vehicle operates at higher altitudes. Thus, the planned sonar data collection survey was given a nominal altitude of 30 m with altitude bounds set at +/- 10 m.

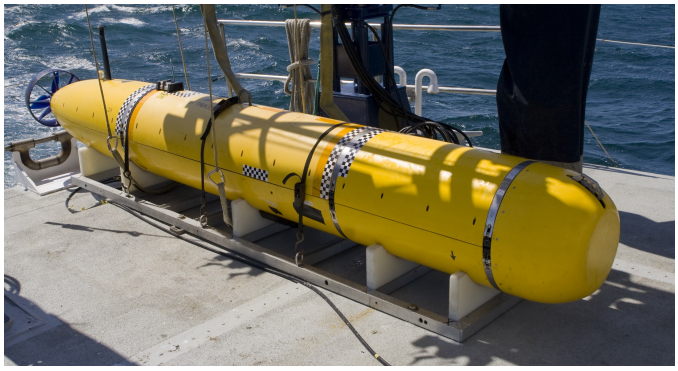

Fig. 10. The MBARI *Dorado* class torpedo-style AUV. The vehicle has a minimum turning radius of 10 m (typical).

The optimization's initial condition was chosen to be a bilinear spline patch with corners coincident with the corners of the bathymetry. Though all attempted initial conditions led to the optimization solver converging to the same answer, the bilinear spline initial condition generally resulted in the optimization converging more quickly.

Trajectories were successfully planned over the Clam Field South terrain data at both survey altitudes. The terrain data for the Clam Field South waypoint is shown in Figure 8. This data set takes the form of a DEM on a 15 m resolution grid. The underlying sonar data was collected using a hull-based sonar survey.

For the 5 m altitude survey, fitting a spline surface to the Clam Field South DEM under the constraints imposed by this trajectory planning method results in the spline surface shown in Figure 11. Due to the curvature constraints, the spline surface is a smoothed version of the terrain. If no constraints were imposed during the spline fitting process, the spline surface would interpolate the bathymetry. Instead, the spline has been smoothed such that trajectories above the

spline surface at an altitude of 5 m comply with the 10 m vehicle turning radius constraint.

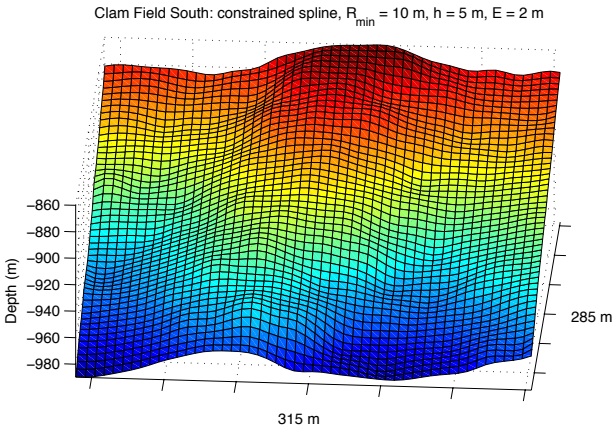

Fig. 11. Spline fit to terrain data under constraints derived from vehicle turning radius.

One example of a survey trajectory computed over the spline surface is shown in Figure 12. Although the trajectory flies over a particularly rough section in the bathymetry, the trajectory smoothly follows the terrain's general shape. Thus, the trajectory yields good instrument-terrain perpendicularity while accounting for the vehicle's turning radius constraint.

Figure 13 shows the curvature, turning radius, and vehicle altitude along the trajectory. The vehicle altitude is the distance between a point on the trajectory and the associated closest point lying on a surface that interpolates the terrain data. The plots show that the trajectory remains within the turning radius constraint and the vehicle altitude bounds.

Similar results were found after executing the trajectory planning method for the 30 m altitude survey of Clam Field South (see Figure 14). The method produced a 30 m altitude survey trajectory that the *Dorado* AUV could drive while keeping the sonar perpendicular to the terrain.

Survey trajectories were also planned over the Soquel Canyon waypoint. Trajectories were successfully planned at 30 m altitude that adhered to the vehicle's turning radius constraint (see Figure 15). However, when a 5 m altitude trajectory was desired, the nonlinear optimization could not fit a spline to the bathymetry within the constraints imposed by a 5 m altitude survey. This failed optimization implies that the *Dorado* would need to violate the +/- 2 m altitude bounds in order to follow the Soquel Canyon terrain within visual range.

V. Conclusion

This paper has presented a method that uses terrain shape information and vehicle actuator constraints to plan feasible terrain following trajectories that maintain instrument-terrain perpendicularity. Using spline surfaces to represent the terrain

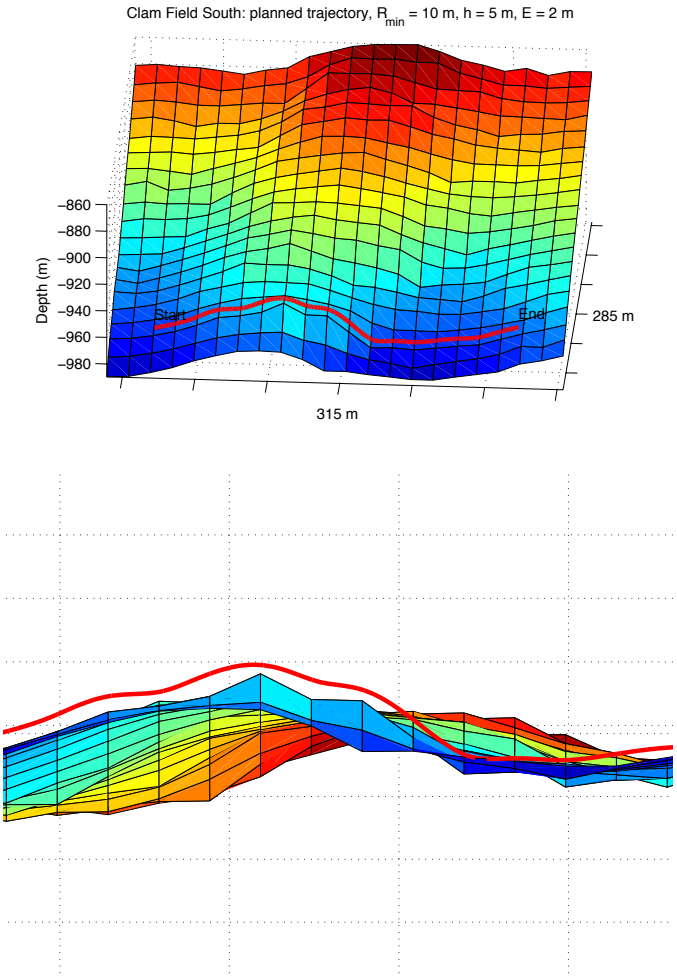

Fig. 12. Two different views of the planned trajectory over Clam Field South plotted over original terrain data.

is a convenient way to enforce curvature constraints on the terrain representation. Since the shape of the vehicle trajectory and spline surface are related via a perpendicularity requirement, the vehicle turning radius constraint can be translated to spline curvature constraints.

The resulting trajectories have shown promise in their ability to adhere to the vehicle turning radius constraint while maintaining perpendicularity to the general shape of the terrain.

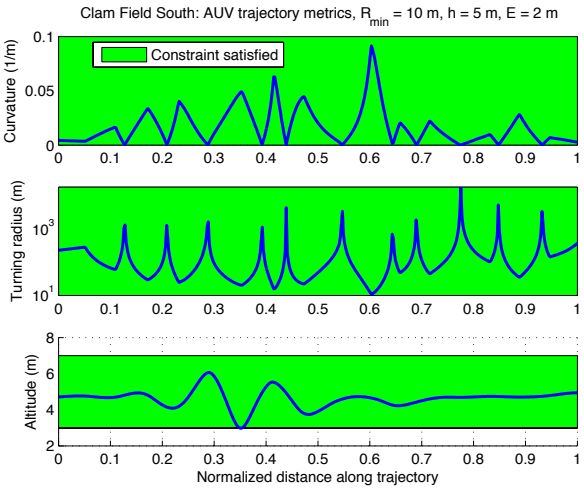

Fig. 13. Trajectory metrics (curvature, altitude). Trajectory remains within the vehicle turning radius constraint and specified altitude bounds.

REFERENCES

[1] D. Caress, H. Thomas, and W. Kirkwood, "High-resolution multibeam, sidescan, and subbottom surveys using the mbari auv d. allan b," *Marine Habitat Mapping Technology for Alaska*, Jan 2008.

[2] H. Singh, R. Eustice, C. Roman, and O. Pizarro, "The seabed auv—a platform for high resolution imaging," *Unmanned Underwater Vehicle Showcase*, 2010.

[3] H. Singh, J. Howland, and O. Pizarro, "Advances in large-area photomosaicking underwater," *IEEE Journal of Oceanic Engineering*, vol. 29, no. 3, pp. 872– 886, 2004.

[4] R. P. Hodges, *Underwater Acoustics: Analysis, Design and Performance of Sonar*. Wiley, Jan 2010.

[5] N. Fairfield, D. Jonak, G. Kantor, and D. Wettergreen, "Field results of the control, navigation, and mapping systems of a hovering auv," in *Proceedings of the 15th International Symposium on Unmanned Untethered Submersible Technology, Durham, NH*, 2007.

[6] N. Fairfield, G. Kantor, and D. Wettergreen, "Real-time slam with octree evidence grids for exploration in underwater tunnels," *Journal of Field Robotics*, vol. 24, no. 1, pp. 3–22, 2007.

[7] A. Kim and R. Eustice, "Pose-graph visual slam with geometric model selection for autonomous underwater ship hull inspection," in *Proceedings of the 2009 IEEE/RSJ International Conference on Intelligent Robots and Systems*, Jan 2009.

[8] K. Murthy and S. Rock, "Performing visual surveys of non-planar benthic terrain," in *Proceedings of Unmanned Untethered Submersible Technology Conference*, 2009.

[9] F. Repoulias and E. Papadopoulos, "Planar trajectory planning and tracking control design for underactuated auvs," *Ocean Engineering*, Jan 2007.

[10] A. Aguiar and J. Hespanha, "Trajectory-tracking and path-following of underactuated autonomous vehicles with parametric modeling uncertainty," *IEEE Transactions on Automatic Control*, Jan 2007.

[11] S. Williams, O. Pizarro, M. Jakuba, and N. Barrett, "Auv benthic habitat mapping in south eastern tasmania," *Field and Service Robotics*, Jan 2010.

[12] N. Tolimieri, M. Clarke, and H. Singh, "Evaluating the seabed auv for monitoring groundfish in untrawlable habitat," *Marine Habitat Mapping Technology for Alaska*, Jan 2008.

[13] H. Singh, R. Armstrong, F. Gilbes, and R. Eustice, "Imaging coral i: Imaging coral habitats with the seabed auv," *Subsurface Sensing Technologies and Applications*, Jan 2004.

[14] I. Nikolos and N. Tsourvelouds, "Path planning for cooperating unmanned vehicles over 3-d terrain," *Informatics in Control*, Jan 2009.

[15] C. Petres, Y. Pailhas, P. Patron, and Y. Petillot, "Path planning for autonomous underwater vehicles," *IEEE Transactions on Robotics*, Jan 2007.

[16] A. Kim and R. Eustice, "Toward auv survey design for optimal coverage and localization using the cramer rao lower bound," in *Proceedings of OCEANS 2009*, 2009.

[17] J. Weekley and D. Brutzman, "Beyond viewpoint: X3d camera nodes for digital cinematography," in *Proceedings of the 14th International Conference on 3D Web Technology*, 2009, pp. 71–77.

[18] J. McCrae, I. Mordatch, M. Glueck, and A. Khan, "Multiscale 3d navigation," in *I3D '09: Proceedings of the 2009 symposium on Interactive 3D graphics and games*, Feb 2009.

[19] A. Khan, B. Komalo, J. Stam, G. Fitzmaurice, and G. Kurtenbach, "Hovercam: interactive 3d navigation for proximal object inspection," in *I3D '05: Proceedings of the 2005 symposium on Interactive 3D graphics and games*, Apr 2005.

[20] A. Hanson and E. Wernert, "Constrained 3d navigation with 2d controllers," in *Proceedings of Visualization '97*, 1997, pp. 175–182.

[21] P. Menon, "Optimal trajectory synthesis for terrain-following flight." *Journal of Guidance, Control, and Dynamics*, vol. 14, no. 4, pp. 807–813, 1991.

[22] R. Hess and Y. Jung, "An application of generalized predictive control to rotorcraft terrain-following flight," *Systems, Man and Cybernetics, IEEE Transactions on DOI - 10.1109/21.44010*, vol. 19, no. 5, pp. 955–962, 1989.

[23] T. Lapp and L. Singh, "Model predictive control based trajectory optimization for nap-of-the-earth (noe) flight including obstacle avoidance," in *Proceedings of the American Control Conference, 2004.*, vol. 1, 2004, pp. 891– 896 vol.1.

[24] L. A. Piegl and W. Tiller, *The NURBS book*. Springer Verlag, Jan 1997.

[25] J. Nocedal and S. Wright, *Numerical optimization*. Springer verlag, 1999.

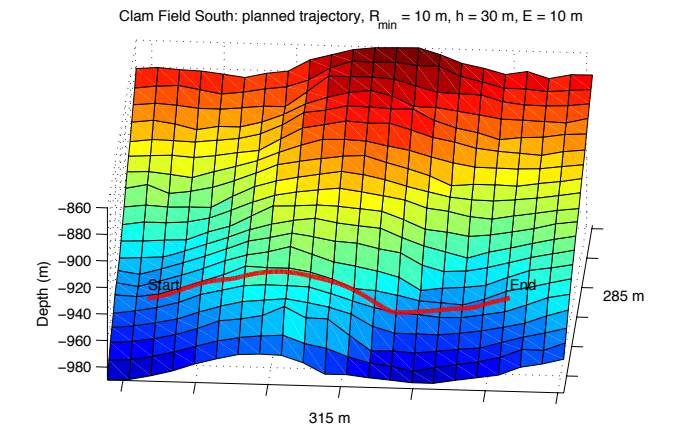

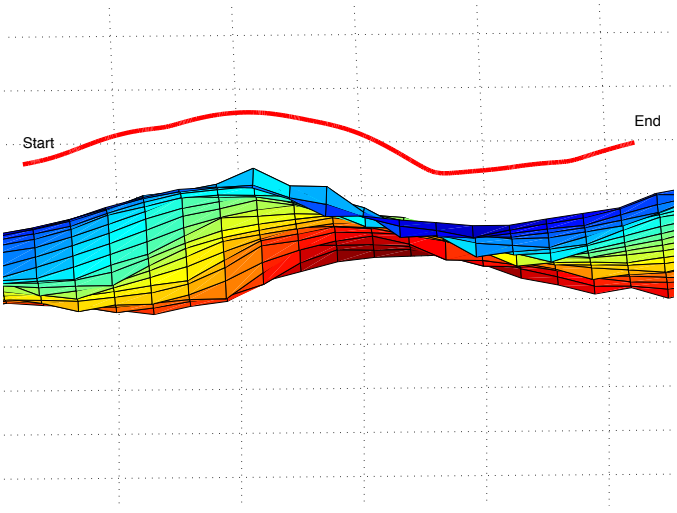

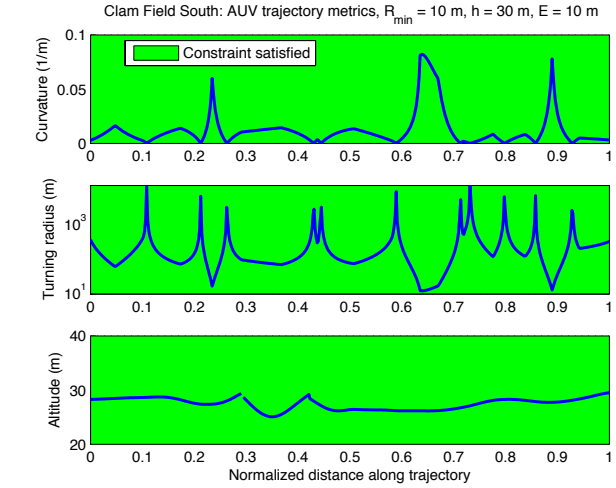

Fig. 14. Planned 30 m altitude survey over Clam Field South. The trajectory metrics show that the trajectory maintains perpendicularity while adhering to the *Dorado*'s turning radius constraint.

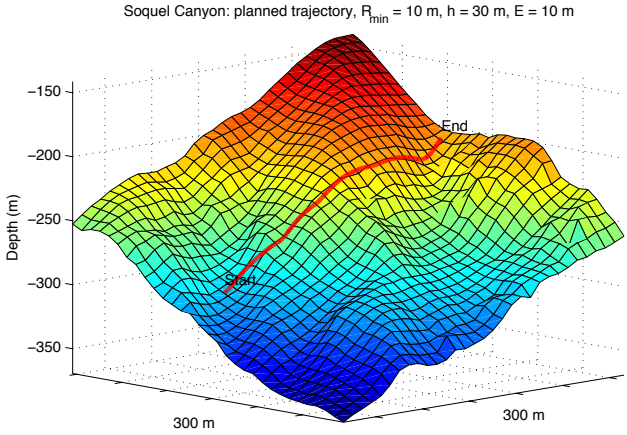

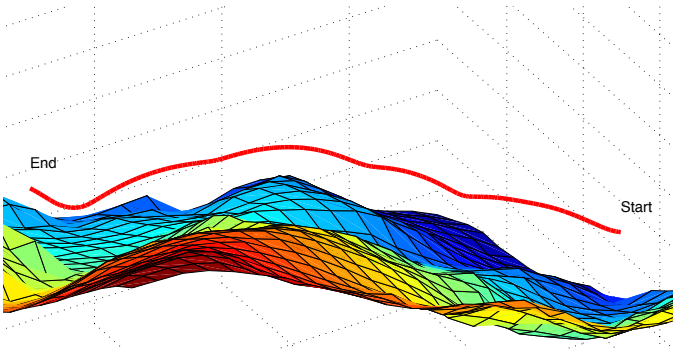

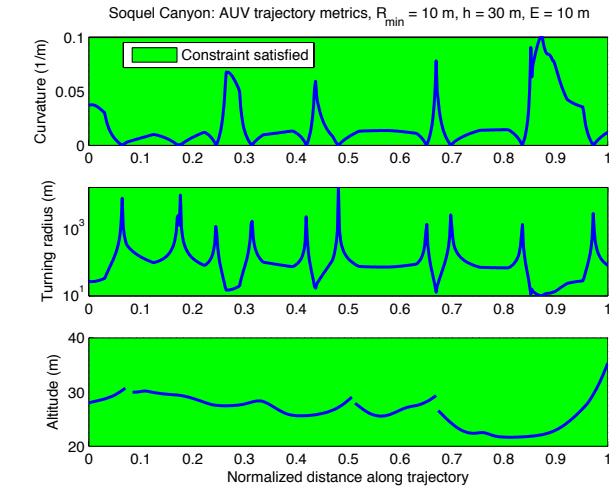

Fig. 15. Two different views of the 30 m altitude planned trajectory over Soquel Canyon, along with associated trajectory metrics.